ACS APPLIED NANO MATERIALS

www.acsanm.org Letter

Nanometer-Thick Sr_2IrO_4 Freestanding Films for Flexible Electronics

Sujan Shrestha, Matthew Coile, Menglin Zhu, Maryam Souri, Jiwoong Kim, Rina Pandey, Joseph W. Brill, Jinwoo Hwang, Jong-Woo Kim, and Ambrose Seo*

Cite This: *ACS Appl. Nano Mater.* 2020, 3, 6310−6315 Read Online

ACCESS | Metrics & More | Article Recommendations | Supporting Information

ABSTRACT: We report the structural and optical properties of nanoscale Sr_2IrO_4 freestanding thin films fabricated using a water-soluble $Sr_3Al_2O_6$ layer. The coherent lattice structure, phonon modes, two-magnon Raman scattering, and optical absorption spectra of the Sr_2IrO_4 nanomembrane are analogous to those of the layered iridate epitaxial thin films and single crystals. Remarkably, the formation of 3-unit-cell-thick $SrIrO_3$ and interfacial composite layers alleviates the antiphase boundaries at the $Sr_2IrO_4/Sr_3Al_2O_6$ interface, resulting in structurally robust nanomembranes. Our experimental results show that this freestanding thin-film approach of layered oxides can provide techniques for tuning or realizing unprecedented states beyond conventional thin-film methods, suggesting a pathway in achieving flexible layered-oxide electronics.

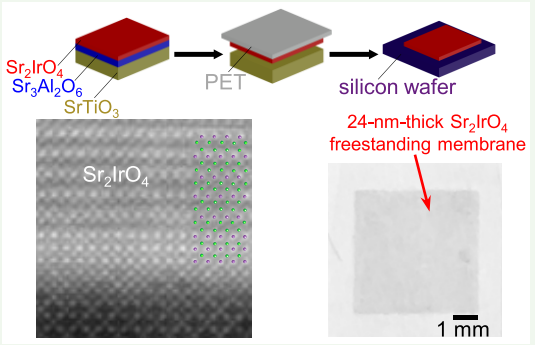

KEYWORDS: *freestanding thin films, layered oxides, Sr_2IrO_4, STEM, interface, strain*

Recently, freestanding metal oxide thin films have attracted attention due to their tunability and potential integration with flexible electronic devices. Constraints imposed by the substrate, such as epitaxial strain and interfacial dislocation, do not play a role in the stand-alone thin films. Therefore, beyond thermodynamic equilibrium, the mechanical modification of freestanding transition metal oxide (TMO) thin films can provide an unprecedented state because their properties are due to strong interactions between charge, spin, and orbital degrees of freedom.[1,2] Hence, freestanding TMO thin films are an ideal system for manipulating and realizing novel devices such as flexible electronics,[1,3−5] ferroelectric memory devices,[6,7] and flexible energy conversion devices[8] by integrating them with semiconductor devices or flexible platforms.

Maintaining the high crystalline quality of freestanding TMO thin film is essential not only for their functional properties but also for device applications. Recently, Lu et al. were able to synthesize high-quality freestanding $SrTiO_3$ and $La_{0.7}Sr_{0.3}MnO_3$ thin films using a water-soluble $Sr_3Al_2O_6$ buffer layer.[9] Note that the perovskites (i.e., AMO_3, where A is an alkaline earth or rare earth element and M is a transition metal element) and $Sr_3Al_2O_6$ have great structural compatibility. However, it is unknown whether the same $Sr_3Al_2O_6$ buffer layer will also work for synthesizing freestanding *layered* oxide (e.g., K_2NiF_4-type structure) thin films. While the in-plane square lattice of layered oxides can match well with that of $Sr_3Al_2O_6$, the large difference in the *c*-axis lattice constant can result in the nucleation of antiphase boundaries[10] near the step-terrace edges of the substrate as shown in Scheme 1. This difference can undermine the structural integrity of the freestanding layered oxide thin films and interfere with its transport to an intended device.

In this letter, we report that 24-nm-thick freestanding thin films of epitaxial Sr_2IrO_4 can be synthesized using a pulsed laser deposition and water-leaching process. Sr_2IrO_4 is a relativistic Mott insulator with the exotic $J_{eff} = 1/2$ pseudospin due to the confluence of strong spin−orbit interaction and electron correlation.[11,12] Due to its structural and magnetic similarities with high-T_c cuprates, this compound has attracted much attention recently.[13−16] We separated a structurally stable freestanding Sr_2IrO_4 thin film from its substrate by dissolving a water-soluble $Sr_3Al_2O_6$ buffer layer, following the description of ref 9. We confirmed the high crystallinity and structural integrity of our freestanding Sr_2IrO_4 thin films, whose quality is comparable to that of epitaxial thin films and single crystals, using various characterization methods. Our results extend the scope of freestanding thin films to the fundamental research and device application of layered oxides such as high-T_c cuprate superconductors.

We grew epitaxial heterostructures of $Sr_2IrO_4/Sr_3Al_2O_6$ on $SrTiO_3$ (0 0 1) substrates using pulsed laser deposition (PLD). Atomically flat surfaces of $SrTiO_3$ (0 0 1) substrates were prepared by deionized-water leaching and thermal annealing,

Received: May 18, 2020
Accepted: July 2, 2020
Published: July 2, 2020

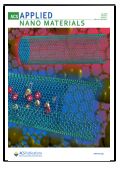

https://dx.doi.org/10.1021/acsanm.0c01351
ACS Appl. Nano Mater. 2020, 3, 6310−6315

Scheme 1. Synthesis of Freestanding Sr_2IrO_4 Membranes by Avoiding the Formation of Antiphase Boundaries on Step Terraces via 3-Unit-Cell $SrIrO_3$ and Interfacial Composite Layers

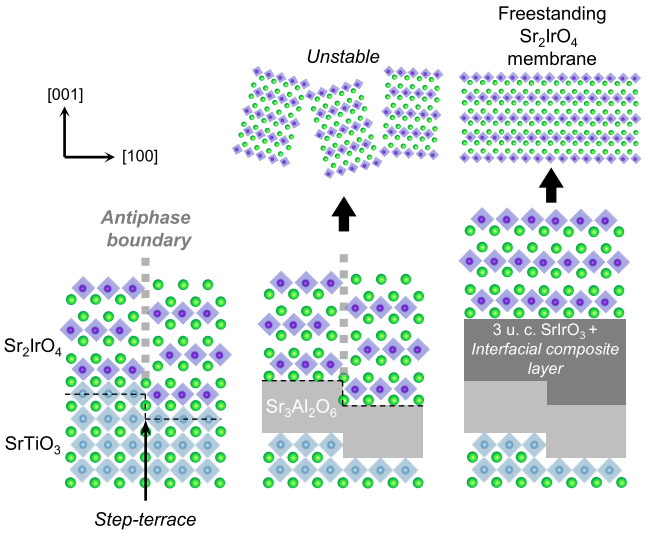

as described in ref 17. We deposited a $Sr_3Al_2O_6$ layer first and then Sr_2IrO_4 epitaxial thin film with K_2NiF_4-type crystal. To stabilize the structure of a Sr_2IrO_4 thin film and facilitate its transport process, we attached a poly(ethylene terephthalate) (PET) film on the sample surface. Following the process described in ref 9, we exfoliated freestanding Sr_2IrO_4 thin film by dissolving the $Sr_3Al_2O_6$ buffer layer in deionized water. Figure 2a shows a photograph of a freestanding Sr_2IrO_4 nanomembrane with the entire area of 5 × 5 mm^2. After this process, we could transfer freestanding thin films into various substrates such as silicon wafers and glass, as shown in Supporting Information Figure S1.

Scanning transmission electron microscopy (STEM) shows that there is a 3-unit-cell-thick $SrIrO_3$ interfacial layer between $Sr_3Al_2O_6$ and Sr_2IrO_4 layers. Figure 1a shows a cross-sectional *Z*-contrast STEM image of an as-grown $Sr_2IrO_4/Sr_3Al_2O_6/SrTiO_3$ sample. High-resolution data of the $Sr_2IrO_4/Sr_3Al_2O_6$ interface (Figure 1b) reveal that there are 3 unit cells of $SrIrO_3$ and an interfacial composite layer between Sr_2IrO_4 and $Sr_3Al_2O_6$, while a sharp interface exists between $Sr_3Al_2O_6$ and $SrTiO_3$ (Figure 1c). Similar interfacial perovskite layers have been observed in various heterointerfaces of complex oxide thin films synthesized by molecular beam epitaxy (MBE) and PLD.[18−21] Note that the interfacial composite layer, which is formed presumably due to the intermixing of $SrIrO_3$ and $Sr_3Al_2O_6$ layers, is only about 2 monolayers thick. Such an atomic-scale interfacial layer has also been observed in the heterointerfaces of $KTaO_3/GdScO_3$ (see ref 22) and

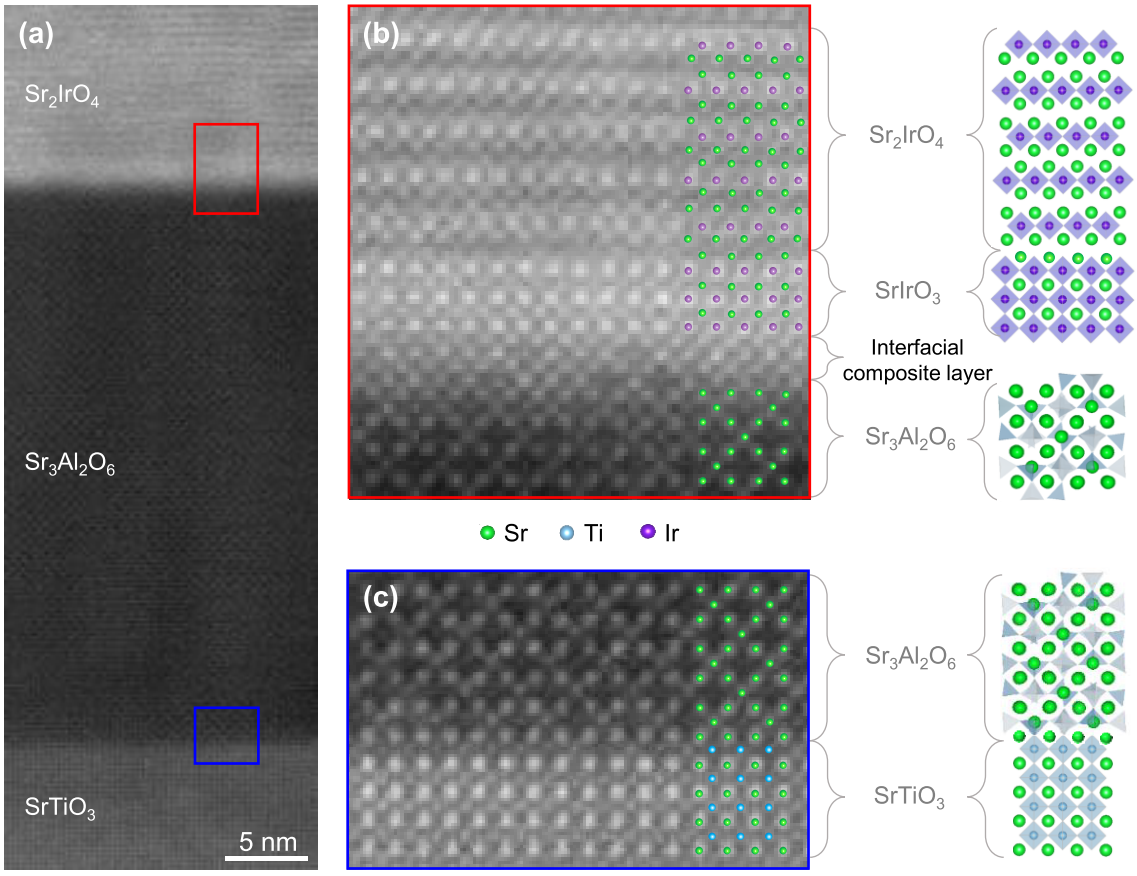

Figure 1. (a) Cross-sectional *Z*-contrast STEM image of an as-grown $Sr_2IrO_4/Sr_3Al_2O_6$ bilayer on a $SrTiO_3$ (001) substrate. High-resolution STEM images of (b) $Sr_2IrO_4/Sr_3Al_2O_6$ (red box) and (c) $Sr_3Al_2O_6/SrTiO_3$ (blue box) interfaces, respectively. The schematic diagram shows microscopic structures obtained from the intensity profiles proportional to the atomic number (*Z*) of each ion. Note that there are an interfacial composite layer and three layers of $SrIrO_3$ at the $Sr_2IrO_4/Sr_3Al_2O_6$ interface. Nevertheless, PLD growth conditions can stabilize epitaxial Sr_2IrO_4 layers on top of the interface.

https://dx.doi.org/10.1021/acsanm.0c01351
ACS Appl. Nano Mater. 2020, 3, 6310−6315

$(La_{0.3}Sr_{0.7})(Al_{0.65}Ta_{0.35})O_3/SrTiO_3$ (see ref 23). These interfacial perovskite and composite layers seem necessary for the thermodynamical stability in many complex oxide heterointerfaces. It is noteworthy that the interfacial composite and 3-unit-cell-thick $SrIrO_3$ layers prevent the formation of any antiphase boundaries in the Sr_2IrO_4 layer, resulting in the high crystallinity of freestanding Sr_2IrO_4 membranes.

X-ray diffraction confirms that the structure of the freestanding Sr_2IrO_4 thin film is coherent. Figure 2b shows

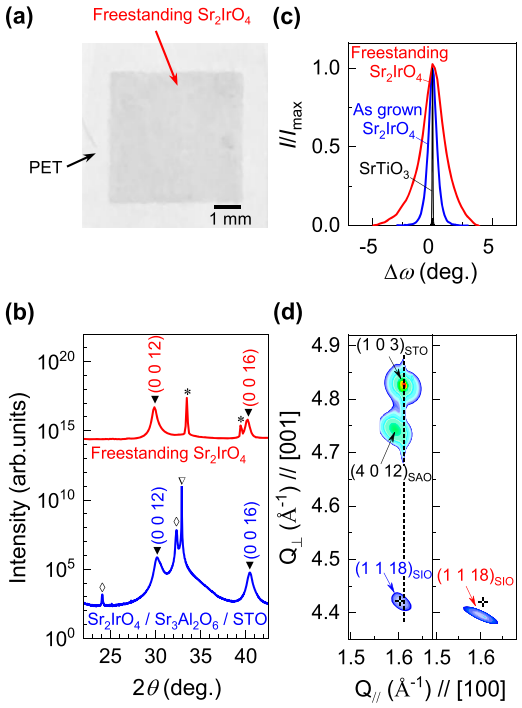

Figure 2. (a) Photograph of a freestanding Sr_2IrO_4 nanomembrane transferred on a poly(ethylene terephthalate) (PET) film. (b) X-ray diffraction $2\theta-\theta$ scans of a $Sr_2IrO_4/Sr_3Al_2O_6/SrTiO_3$ sample and a freestanding Sr_2IrO_4 membrane transferred to a silicon wafer. Symbols ▼ and ◊ indicate the peaks from the Sr_2IrO_4 thin film and the $Sr_3Al_2O_6$ layer, respectively. Asterisks (*) and symbol ▽ indicate peaks from the substrates, i.e., silicon and $SrTiO_3$, respectively. (c) X-ray rocking curves of a freestanding Sr_2IrO_4 thin film on silicon and an as-grown $Sr_2IrO_4/Sr_3Al_2O_6/SrTiO_3$. The increased fwhm of the freestanding Sr_2IrO_4 thin film (2.11°) compared to the as-grown Sr_2IrO_4 thin film (0.84°) implies that mosaicity increases during the transfer process. (d) X-ray reciprocal space mapping of as-grown $Sr_2IrO_4/Sr_3Al_2O_6/SrTiO_3$ and a freestanding Sr_2IrO_4 thin film near the (1 0 3) reflection of $SrTiO_3$. Both samples clearly show the (1 1 18) reflection of Sr_2IrO_4. The cross symbol indicates the peak position of the as-grown $Sr_2IrO_4/Sr_3Al_2O_6/SrTiO_3$ for comparison with the freestanding Sr_2IrO_4 thin film.

the $2\theta-\theta$ scans of a 24-nm-thick freestanding Sr_2IrO_4 membrane placed on a silicon wafer and a $Sr_2IrO_4/Sr_3Al_2O_6/SrTiO_3$ sample. Well-defined (0 0 l) peaks from Sr_2IrO_4 are presented in both samples, while the freestanding Sr_2IrO_4 thin film does not show any peaks from $Sr_3Al_2O_6$ or $SrTiO_3$. However, the broad full width at half-maximum of the rocking curve (Figure 2c) indicates that the freestanding Sr_2IrO_4 thin film has more mosaic spread than the as-grown Sr_2IrO_4 thin film on $Sr_3Al_2O_6/SrTiO_3$, presumably due to structural degradation during the exfoliation and transfer processes.[24] Nevertheless, the single peak rocking curve indicates that multiple domains are not present. We obtained the in-plane and out-of-plane lattice parameters from X-ray reciprocal space mapping (RSM), as shown in Figure 2d, near the (1 0 3) reflection of $SrTiO_3$ substrates. Clear (1 1 18) and (4 0 12) reflections are visible from Sr_2IrO_4 and $Sr_3Al_2O_6$, respectively. From these RSM data, we can see that the as-grown Sr_2IrO_4 thin film is under tensile strain although the $Sr_3Al_2O_6$ buffer layer is partially relaxed. The freestanding Sr_2IrO_4 thin film has a longer c-axis lattice constant than the as-grown Sr_2IrO_4 thin film while their in-plane lattice constants are similar to each other. Table 1 shows the in-plane and out-of-plane lattice constants and strain values ε_{xx} and ε_{zz}. Note that the freestanding Sr_2IrO_4 thin film is under tensile strain, i.e., larger in-plane lattice and smaller out-of-plane lattice than Sr_2IrO_4 single crystals, presumably due to a small number of defects such as oxygen vacancies created during the sample synthesis.

Polarization-dependent Raman spectroscopy shows that the lattice dynamics of the freestanding Sr_2IrO_4 membrane is consistent with that of Sr_2IrO_4 epitaxial thin films and single crystals. Figure 3a shows Raman spectra of a freestanding Sr_2IrO_4 thin film on a PET film measured at room temperature with $z(x'y')\bar{z}$ (B_{1g}), $z(x'x')\bar{z}$ (A_{1g} + B_{2g}), $z(xy)\bar{z}$ (B_{2g}), and $z(xx)\bar{z}$ (A_{1g} + B_{1g}) scattering geometries. The axes x' and y' are directed along the Ir−O bond direction and x and y axes are rotated 45° relative to them. The observed phonon modes are consistent with those of $Sr_2IrO_4/SrTiO_3$ thin films and Sr_2IrO_4 single crystals, reported in refs 25−27. Figure 3b shows the temperature-dependent B_{2g} mode spectra of a freestanding Sr_2IrO_4 membrane on a silicon wafer. At low temperature, a broad two-magnon scattering peak emerges and its peak energy (ω_{2M}) is approximately 1330 cm^{-1} at 10 K. The overall spectral shape of the two-magnon scattering is consistent with that of Sr_2IrO_4 epitaxial thin films and single crystals.[25,28] The measured ω_{2M} value implies that the exchange interaction (J) of the J_{eff} = 1/2 pseudospins in our freestanding Sr_2IrO_4 thin film is approximately 60 meV.

From optical spectroscopic measurements (Figure 4), we observed a blue-shifted J_{eff} = 1/2 interband optical transition, implying that slight tensile strain exists in our freestanding Sr_2IrO_4 thin film. Both as-grown and freestanding Sr_2IrO_4 thin films show a well-known two-peak structure, marked as α and β, in their optical absorption spectra, which is consistent with the previously reported data of Sr_2IrO_4 thin films and single crystals.[29−31] The overall optical absorption in the photon energies below 2 eV is due to the interband optical transitions from the lower Hubbard band (LHB) to the upper Hubbard

Table 1. In-Plane and Out-of-Plane Lattice Constants and Strain Values of As-Grown Sr_2IrO_4 and Freestanding Sr_2IrO_4 Thin Films[a]

	a (Å)	c (Å)	ε_{xx} (%)	ε_{zz} (%)	Poisson ratio
as-grown Sr_2IrO_4	5.54	25.50	+0.73 ± 0.16	−1.12 ± 0.16	0.49 ± 0.20
freestanding Sr_2IrO_4	5.53	25.74	+0.55 ± 0.35	−0.18 ± 0.06	0.26 ± 0.20

[a] $\varepsilon_{xx} = (a_{film} - a_{bulk})/a_{bulk} \times 100$ (%), and $\varepsilon_{zz} = (c_{film} - c_{bulk})/c_{bulk} \times 100$ (%).

https://dx.doi.org/10.1021/acsanm.0c01351
ACS Appl. Nano Mater. 2020, 3, 6310−6315

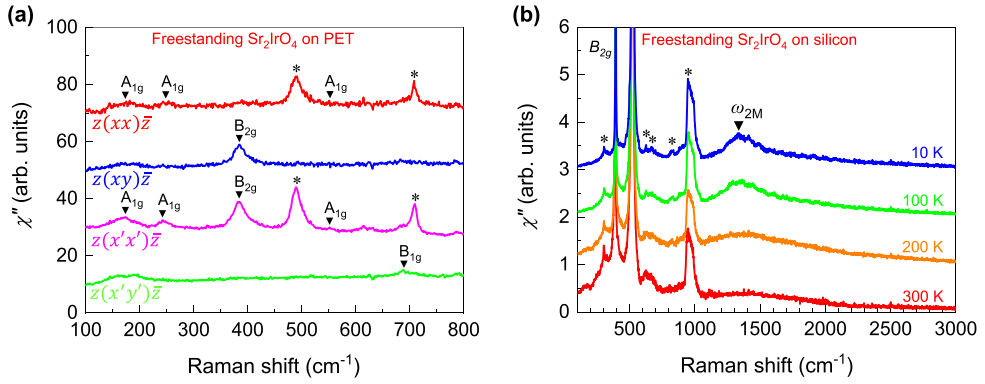

Figure 3. (a) Polarization-dependent Raman spectra of a 24 nm thick freestanding Sr_2IrO_4 membrane sitting on a PET membrane at room temperature. Four polarization-dependent backscattering channels $z(xx)\bar{z}$, $z(xy)\bar{z}$, $z(x'x')\bar{z}$, and $z(x'y')\bar{z}$ probe A_{1g} + B_{1g}, B_{2g}, A_{1g} + B_{2g}, and B_{1g} modes, respectively. The polarization-dependent phonon modes of the freestanding Sr_2IrO_4 thin film is consistent with epitaxial thin films and single crystals of Sr_2IrO_4.[25−27] Asterisks (*) indicate molecular vibrations from PET. (b) Temperature-dependent B_{2g} mode Raman spectra of a freestanding Sr_2IrO_4 thin film transferred on a silicon wafer. Symbol ▼ (1335 cm^{-1}) indicates a two-magnon scattering peak of the Sr_2IrO_4 freestanding thin film. The sharp peak around 395 cm^{-1} is a B_{2g} phonon of Sr_2IrO_4. Asterisks (*) indicate phonon modes of silicon.

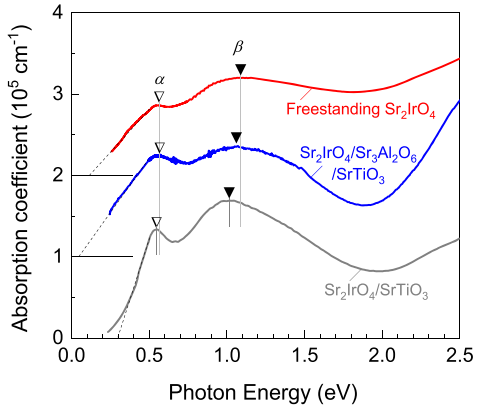

Figure 4. Optical absorption coefficient spectra of freestanding Sr_2IrO_4 thin films and $Sr_2IrO_4/Sr_3Al_2O_6/SrTiO_3$ samples. The spectrum of an epitaxial Sr_2IrO_4 thin film grown on a $SrTiO_3$ substrate is shown for comparison from ref 29. The spectra are vertically shifted for clarity.

band (UHB) of the J_{eff} = 1/2 state.[32] Note that the optical absorption spectrum of the freestanding Sr_2IrO_4 thin film is broader and shifted slightly to higher energies than the $Sr_2IrO_4/SrTiO_3$ sample reported in ref 29. This observation is consistent with the X-ray diffraction data (Figure 2) because the broad and blue-shifted optical absorption spectrum is relevant to the increased Ir−O−Ir bond angle of the freestanding Sr_2IrO_4 thin films.

In conclusion, we synthesized high-quality freestanding Sr_2IrO_4 nanomembranes using water-soluble $Sr_3Al_2O_6$ and conducted structural and optical characterizations of the samples. We observed coherent lattice structure, phonon modes, two-magnon Raman scattering, and optical absorption spectra of the freestanding Sr_2IrO_4 thin film. While there is a slight degradation of crystallinity and some generic tensile strain, the overall properties of the freestanding Sr_2IrO_4 thin film are analogous to those of the layered iridate epitaxial thin films and single crystals. Note that 3-unit-cell-thick $SrIrO_3$ and interfacial composite layers play an important role in avoiding the formation of antiphase boundaries at the heterointerface between the layered iridate and $Sr_3Al_2O_6$ and protect the structural integrity of the freestanding Sr_2IrO_4 thin film. We suggest that freestanding thin films of layered oxides with strongly correlated electrons can be a model system for tuning their physical properties beyond the thermodynamic limit of materials by combining them with piezoelectric or mechanical strain devices. Our results extend the scope of freestanding thin films to the fundamental research beyond conventional thin films and device application of layered oxides by integrating them with the semiconductor devices and flexible platforms.

■ ASSOCIATED CONTENT

Supporting Information

The Supporting Information is available free of charge at https://pubs.acs.org/doi/10.1021/acsanm.0c01351.

Synthesis and characterization, schematic diagrams of the freestanding Sr_2IrO_4 thin film, and optical transmission spectra of a freestanding Sr_2IrO_4 thin film on PET and an as-grown $Sr_2IrO_4/Sr_3Al_2O_6$ layer on a $SrTiO_3$ substrate (PDF)

■ AUTHOR INFORMATION

Corresponding Author

Ambrose Seo − *Department of Physics and Astronomy, University of Kentucky, Lexington, Kentucky 40506, United States;* orcid.org/0000-0002-7055-5314; Email: a.seo@uky.edu

Authors

Sujan Shrestha − *Department of Physics and Astronomy, University of Kentucky, Lexington, Kentucky 40506, United States*

Matthew Coile − *Department of Physics and Astronomy, University of Kentucky, Lexington, Kentucky 40506, United States*

Menglin Zhu − *Department of Materials Science and Engineering, The Ohio State University, Columbus, Ohio 43210, United States*

Maryam Souri − *Department of Physics and Astronomy, University of Kentucky, Lexington, Kentucky 40506, United States*

Jiwoong Kim − *Department of Physics and Astronomy, University of Kentucky, Lexington, Kentucky 40506, United States; Department of Physics, Pusan National University, Busan 46241, South Korea*

https://dx.doi.org/10.1021/acsanm.0c01351
ACS Appl. Nano Mater. 2020, 3, 6310−6315

Rina Pandey − *Department of Physics and Astronomy, University of Kentucky, Lexington, Kentucky 40506, United States*

Joseph W. Brill − *Department of Physics and Astronomy, University of Kentucky, Lexington, Kentucky 40506, United States*

Jinwoo Hwang − *Department of Materials Science and Engineering, The Ohio State University, Columbus, Ohio 43210, United States*

Jong-Woo Kim − *Advanced Photon Source, Argonne National Laboratory, Argonne, Illinois 60439, United States*

Complete contact information is available at: https://pubs.acs.org/10.1021/acsanm.0c01351

Notes

The authors declare no competing financial interest.

■ ACKNOWLEDGMENTS

We acknowledge the support of a National Science Foundation (NSF) Grant No. DMR-1454200 for thin-film synthesis and characterization. M.Z. and J.H. acknowledge support by NSF, under Grant No. DMR-1847964. Electron microscopy was performed at the Center for Electron Microscopy and Analysis at The Ohio State University. This research used resources of the Advanced Photon Source, a U.S. Department of Energy (DOE) Office of Science User Facility operated for the DOE Office of Science by Argonne National Laboratory under Contract No. DE-AC02-06CH11357. A.S. acknowledges the support from the Alexander von Humboldt Foundation (Research Fellowship for Experienced Researchers) for Raman spectroscopy experiments.

■ REFERENCES

(1) Zhang, Y.; Ma, C.; Lu, X.; Liu, M. Recent progress on flexible inorganic single-crystalline functional oxide films for advanced electronics. *Mater. Horiz.* **2019**, *6* (5), 911−930.

(2) Hwang, H. Y.; Iwasa, Y.; Kawasaki, M.; Keimer, B.; Nagaosa, N.; Tokura, Y. Emergent phenomena at oxide interfaces. *Nat. Mater.* **2012**, *11* (2), 103−113.

(3) Ahn, J.-H.; Je, J. H. Stretchable electronics: materials, architectures and integrations. *J. Phys. D: Appl. Phys.* **2012**, *45* (10), 103001.

(4) Rogers, J. A.; Lagally, M. G.; Nuzzo, R. G. Synthesis, assembly and applications of semiconductor nanomembranes. *Nature* **2011**, *477* (7362), 45−53.

(5) Paskiewicz, D. M.; Sichel-Tissot, R.; Karapetrova, E.; Stan, L.; Fong, D. D. Single-Crystalline SrRuO3 Nanomembranes: A Platform for Flexible Oxide Electronics. *Nano Lett.* **2016**, *16* (1), 534−542.

(6) Lu, D.; Crossley, S.; Xu, R.; Hikita, Y.; Hwang, H. Y. Freestanding Oxide Ferroelectric Tunnel Junction Memories Transferred onto Silicon. *Nano Lett.* **2019**, *19* (6), 3999−4003.

(7) Bakaul, S. R.; Serrao, C. R.; Lee, O.; Lu, Z.; Yadav, A.; Carraro, C.; Maboudian, R.; Ramesh, R.; Salahuddin, S. High Speed Epitaxial Perovskite Memory on Flexible Substrates. *Adv. Mater.* **2017**, *29* (11), 1605699.

(8) Qi, Y.; Jafferis, N. T.; Lyons, K.; Lee, C. M.; Ahmad, H.; McAlpine, M. C. Piezoelectric Ribbons Printed onto Rubber for Flexible Energy Conversion. *Nano Lett.* **2010**, *10* (2), 524−528.

(9) Lu, D.; Baek, D. J.; Hong, S. S.; Kourkoutis, L. F.; Hikita, Y.; Hwang, H. Y. Synthesis of freestanding single-crystal perovskite films and heterostructures by etching of sacrificial water-soluble layers. *Nat. Mater.* **2016**, *15* (12), 1255−1260.

(10) Wang, Z.; Guo, H.; Shao, S.; Saghayezhian, M.; Li, J.; Fittipaldi, R.; Vecchione, A.; Siwakoti, P.; Zhu, Y.; Zhang, J.; Plummer, E. W. Designing antiphase boundaries by atomic control of heterointerfaces. *Proc. Natl. Acad. Sci. U. S. A.* **2018**, *115* (38), 9485.

(11) Kim, B. J.; Jin, H.; Moon, S. J.; Kim, J. Y.; Park, B. G.; Leem, C. S.; Yu, J.; Noh, T. W.; Kim, C.; Oh, S. J.; Park, J. H.; Durairaj, V.; Cao, G.; Rotenberg, E. Novel Jeff = 1/2 Mott State Induced by Relativistic Spin-Orbit Coupling in Sr2IrO4. *Phys. Rev. Lett.* **2008**, *101* (7), 076402.

(12) Kim, B. J.; Ohsumi, H.; Komesu, T.; Sakai, S.; Morita, T.; Takagi, H.; Arima, T. Phase-Sensitive Observation of a Spin-Orbital Mott State in Sr2IrO4. *Science* **2009**, *323* (5919), 1329.

(13) Kim, J.; Casa, D.; Upton, M. H.; Gog, T.; Kim, Y.-J.; Mitchell, J. F.; van Veenendaal, M.; Daghofer, M.; van den Brink, J.; Khaliullin, G.; Kim, B. J. Magnetic Excitation Spectra of Sr2IrO4 Probed by Resonant Inelastic X-Ray Scattering: Establishing Links to Cuprate Superconductors. *Phys. Rev. Lett.* **2012**, *108* (17), 177003.

(14) Fujiyama, S.; Ohsumi, H.; Komesu, T.; Matsuno, J.; Kim, B. J.; Takata, M.; Arima, T.; Takagi, H. Two-Dimensional Heisenberg Behavior of Jeff = 1/2 Isospins in the Paramagnetic State of the Spin-Orbital Mott Insulator Sr2IrO4. *Phys. Rev. Lett.* **2012**, *108* (24), 247212.

(15) Wang, F.; Senthil, T. Twisted Hubbard Model for Sr2IrO4: Magnetism and Possible High Temperature Superconductivity. *Phys. Rev. Lett.* **2011**, *106* (13), 136402.

(16) Watanabe, H.; Shirakawa, T.; Yunoki, S. Monte Carlo Study of an Unconventional Superconducting Phase in Iridium Oxide Jeff = 1/2 Mott Insulators Induced by Carrier Doping. *Phys. Rev. Lett.* **2013**, *110* (2), 027002.

(17) Connell, J. G.; Isaac, B. J.; Ekanayake, G. B.; Strachan, D. R.; Seo, S. S. A. Preparation of atomically flat SrTiO3 surfaces using a deionized-water leaching and thermal annealing procedure. *Appl. Phys. Lett.* **2012**, *101* (25), 251607.

(18) Seo, S. S. A.; Nichols, J.; Hwang, J.; Terzic, J.; Gruenewald, J. H.; Souri, M.; Thompson, J.; Connell, J. G.; Cao, G. Selective growth of epitaxial Sr2IrO4 by controlling plume dimensions in pulsed laser deposition. *Appl. Phys. Lett.* **2016**, *109* (20), 201901.

(19) Lee, J. H.; Luo, G.; Tung, I. C.; Chang, S. H.; Luo, Z.; Malshe, M.; Gadre, M.; Bhattacharya, A.; Nakhmanson, S. M.; Eastman, J. A.; Hong, H.; Jellinek, J.; Morgan, D.; Fong, D. D.; Freeland, J. W. Dynamic layer rearrangement during growth of layered oxide films by molecular beam epitaxy. *Nat. Mater.* **2014**, *13* (9), 879−883.

(20) Nie, Y. F.; Zhu, Y.; Lee, C. H.; Kourkoutis, L. F.; Mundy, J. A.; Junquera, J.; Ghosez, P.; Baek, D. J.; Sung, S.; Xi, X. X.; Shen, K. M.; Muller, D. A.; Schlom, D. G. Atomically precise interfaces from non-stoichiometric deposition. *Nat. Commun.* **2014**, *5* (1), 4530.

(21) Choi, W. S.; Kwon, J.-H.; Jeen, H.; Hamann-Borrero, J. E.; Radi, A.; Macke, S.; Sutarto, R.; He, F.; Sawatzky, G. A.; Hinkov, V.; Kim, M.; Lee, H. N. Strain-Induced Spin States in Atomically Ordered Cobaltites. *Nano Lett.* **2012**, *12* (9), 4966−4970.

(22) Thompson, J.; Hwang, J.; Nichols, J.; Connell, J. G.; Stemmer, S.; Seo, S. S. A. Alleviating polarity-conflict at the heterointerfaces of KTaO3/GdScO3 polar complex-oxides. *Appl. Phys. Lett.* **2014**, *105* (10), 102901.

(23) Huang, Z.; Han, K.; Zeng, S.; Motapothula, M.; Borisevich, A. Y.; Ghosh, S.; Lü, W.; Li, C.; Zhou, W.; Liu, Z.; Coey, M.; Venkatesan, T.; Ariando. The Effect of Polar Fluctuation and Lattice Mismatch on Carrier Mobility at Oxide Interfaces. *Nano Lett.* **2016**, *16* (4), 2307−2313.

(24) McCarthy, E.; Rajendra Kumar, R. T.; Doggett, B.; Chakrabarti, S.; O'Haire, R. J.; Newcomb, S. B.; Mosnier, J. P.; Henry, M. O.; McGlynn, E. Effects of the crystallite mosaic spread on integrated peak intensities in $2\theta-\omega$ measurements of highly crystallographically textured ZnO thin films. *J. Phys. D: Appl. Phys.* **2011**, *44* (37), 375401.

(25) Seo, A.; Stavropoulos, P. P.; Kim, H. H.; Fürsich, K.; Souri, M.; Connell, J. G.; Gretarsson, H.; Minola, M.; Kee, H. Y.; Keimer, B. Compressive strain induced enhancement of exchange interaction and short-range magnetic order in Sr2IrO4 investigated by Raman spectroscopy. *Phys. Rev. B: Condens. Matter Mater. Phys.* **2019**, *100* (16), 165106.

(26) Cetin, M. F.; Lemmens, P.; Gnezdilov, V.; Wulferding, D.; Menzel, D.; Takayama, T.; Ohashi, K.; Takagi, H. Crossover from coherent to incoherent scattering in spin-orbit dominated Sr2IrO4. *Phys. Rev. B: Condens. Matter Mater. Phys.* **2012**, *85* (19), 195148.
(27) Gretarsson, H.; Sauceda, J.; Sung, N. H.; Höppner, M.; Minola, M.; Kim, B. J.; Keimer, B.; Le Tacon, M. Raman scattering study of vibrational and magnetic excitations in $Sr_{2-x}La_xIrO_4$. *Phys. Rev. B: Condens. Matter Mater. Phys.* **2017**, *96* (11), 115138.
(28) Gretarsson, H.; Sung, N. H.; Höppner, M.; Kim, B. J.; Keimer, B.; Le Tacon, M. Two-Magnon Raman Scattering and Pseudospin-Lattice Interactions in Sr2IrO4 and Sr3Ir2O7. *Phys. Rev. Lett.* **2016**, *116* (13), 136401.
(29) Nichols, J.; Terzic, J.; Bittle, E. G.; Korneta, O. B.; De Long, L. E.; Brill, J. W.; Cao, G.; Seo, S. S. A. Tuning electronic structure via epitaxial strain in Sr2IrO4 thin films. *Appl. Phys. Lett.* **2013**, *102* (14), 141908.
(30) Moon, S. J.; Jin, H.; Choi, W. S.; Lee, J. S.; Seo, S. S. A.; Yu, J.; Cao, G.; Noh, T. W.; Lee, Y. S. Temperature dependence of the electronic structure of the Jeff = 1/2 Mott insulator Sr2IrO4 studied by optical spectroscopy. *Phys. Rev. B: Condens. Matter Mater. Phys.* **2009**, *80* (19), 195110.
(31) Kim, B. H.; Khaliullin, G.; Min, B. I. Magnetic Couplings, Optical Spectra, and Spin-Orbit Exciton in 5d Electron Mott Insulator Sr2IrO4. *Phys. Rev. Lett.* **2012**, *109* (16), 167205.
(32) Souri, M.; Kim, B. H.; Gruenewald, J. H.; Connell, J. G.; Thompson, J.; Nichols, J.; Terzic, J.; Min, B. I.; Cao, G.; Brill, J. W.; Seo, A. Optical signatures of spin-orbit exciton in bandwidth-controlled Sr2IrO4 epitaxial films via high-concentration Ca and Ba doping. *Phys. Rev. B: Condens. Matter Mater. Phys.* **2017**, *95* (23), 235125.

https://dx.doi.org/10.1021/acsanm.0c01351
ACS Appl. Nano Mater. 2020, 3, 6310−6315